https://doi.org/10.26565/2220-637X-2023-41-01 ISSN 2220-637X
УДК: 004.94 + 54-145.4 + 544.034.1 + 544.272 + 544.623

MOLECULAR DYNAMICS STUDY OF IMIDAZOLIUM IONIC LIQUIDS AND MOLECULAR SOLVENTS: INSIGHTS INTO MICROSTRUCTURE AND TRANSPORT PHENOMENA

D.S. Dudariev[*,†,a], Y.V. Kolesnik[*,b], A. Idrissi[†,c], O.N. Kalugin[*,d]

[*]*V. N. Karazin Kharkiv National University, School of Chemistry, 4 Svobody sqr., Kharkiv, 61022 Ukraine*

[†]*University of Lille, CNRS UMR 8516 -LASIRe - Laboratoire Avancé de Spectroscopie pour les Interactions la Réactivité et l'environnement, 59000 Lille, France*

a) dimadudariev@gmail.com https://orcid.org/0000-0002-2556-8036
b) ykolesnik@karazin.ua https://orcid.org/0000-0002-9569-4556
c) nacer.idrissi@univ-lille1.fr https://orcid.org/0000-0002-6924-6434
d) onkalugin@gmail.com https://orcid.org/0000-0003-3273-9259

Binary mixtures composed of room-temperature ionic liquids and aprotic dipolar solvents are widely used in the modern electrochemistry. While these systems exhibit maximum electroconductivity and other changes in diluted solutions, as confirmed by NMR and vibrational spectroscopic data, there is currently no theory that can fully explain these phenomena. In current work twelve mixtures of ionic liquids (ILs), in particular 1-butyl-3-methylimdazolium (C_4mim^+) with tetrafluoroborate (BF_4^-), hexafluorophosphate (PF_6^-), trifluoromethanesulfonate (TFO^-) and bis(trifluoromethane)sulfonimide ($TFSI^-$) with molecular solvents such as acetonitrile (AN), propylene carbonate (PC) or gamma butyrolactone (γ-BL) were studied by the molecular dynamics simulation technique. The local structure of the mixtures was studied in the framework of radial distribution functions (RDFs) and running coordination numbers (RCNs) that showed the particular behavior in AN and $TFSI^-$ systems. For $TFSI^-$ system the presence of two peaks on the RDFs with similar intensities were observed. The mutual arrangement of cation and anion corresponding to observed on the RDFs interatomic distances were investigated: they represent the position when the nitrogen atom of the anion is close to the imidazolium ring and when nitrogen atom of TFSI- not directly interacting with the ring, but instead the oxygen atoms do. The cation-anion coordination numbers changed for mixtures with AN from ~1.2 to ~3.6, for PC – from 0.6 to 3.0 and for γ-BL – from 0.8 to 3.1 with the increasing mole fraction of the ILs. Also, the association analysis was conducted using two different distance criteria. The results showed the formation of large clusters at approximately 0.15, 0.20, and 0.25 IL mole fractions for AN, PC, and γ-BL, respectively, based on the first criterion. However, this criterion tends to overestimate the extent of aggregation. In contrast, the second, stricter criterion indicates that the formation of large aggregates begins at IL mole fractions similar to where the experimental conductivity curves reach their maximum. To analyze the transport properties the diffusion coefficients of all the components and shear viscosity for all binary mixtures were obtained. The diffusion coefficients show good agreement with experimental data.

Keywords: *1-butyl-3-methylimdazolium, ionic liquids, aprotic dipolar solvents, local structure, transport properties, ionic aggregation*

Introduction

Ionic liquid (IL) mixtures with molecular solvents can be considered as electrolyte solutions, for which their structure and properties are determined by the balance of types of interactions between all particles in the solution (cation, anion and solvent), which determine the existence of ionic associates and high-order aggregates . In this context, the main feature of binary systems based on IL is that the constituent ions are polyatomic and, as a rule, asymmetric. As a result, the interactions mentioned above should be considered as anisotropic, having a predominant localization around some molecular fragment (center of interaction) . Another important feature of these systems in comparison with ordinary solutions of electrolytes is the complete miscibility of IL with many molecular solvents, which makes it possible to obtain mixtures corresponding to either a solution of such a liquid in a molecular solvent or a solution of a molecular solvent in an ionic liquid.

Intermolecular interactions in mixtures of two liquids of different nature can be showed as a gradual transition from the “first pure liquid” to the “second pure liquid” through intermediate

© Dudariev D. S., Kolesnik Y. V., Idrissi A., Kalugin O. N., 2023
This is an open access article distributed under the terms of the Creative Commons Attribution License 4.0.

compositions. Thus, the task boils down to the following question: which ranges of composition correspond to the above-mentioned areas, and which intermolecular interactions are decisive .

For pure ILs, there is currently no generally accepted picture of their structure due to the indirect nature of the methods used. It is widely believed that in the liquid state the structure of imidazolium ionic liquids is determined by strong interionic Coulomb interactions, which are relatively effectively shielded away from the central ion (i.e., are quite local). It is also assumed that a significant contribution is made by the three-dimensional network of hydrogen bonds between counterions . The strength and structure of this network are determined by the nature (polarizability, polarizing action, size, etc.) of the anion .

The above-mentioned considerations about the structure of pure components indicate the presence of two main phenomena in which a redistribution of the equilibrium between possible ion-ion, ion-molecular and intermolecular interactions can be manifested when the composition changes. These are ionic association and ionic solvation .

These phenomena can be explained as the gradual breakdown of large ionic aggregates, which are the fundamental structural units of pure ionic liquids, into smaller aggregates and eventually into ion pairs. This process occurs as the system transitions from a concentrated ionic liquid to a more dilute solution. In dilute solutions, ion pairs completely dissociate into "free" ions due to interactions with the solvent. These interactions can be specific, involving localized ion-molecular interactions, or non-specific, resulting from the presence of a large amount of solvent that creates an environment similar to that of a pure solvent. .

The phenomena of ionic association and solvation are manifested at the microscopic level in the redistribution of electron density in the corresponding areas of interaction and, therefore, in changes in the corresponding force constants. Among the currently known experimental methods that can detect such effects, NMR and vibrational (IR and Raman) spectroscopy should be singled out. The first can reveal information about the change in the electronic microenvironment of each chemically non-equivalent nucleus and the relative location for some nuclei, while the second investigates changes in the constants of the dipole moment, polarizability, changes in the microenvironment of atoms participating in the studied vibrational mode .

The association and solvation are also reflected in the “statistical” microstructure of such binary mixtures. Currently, only various methods of diffraction of X-rays and neutrons can provide experimental data on the such microstructure in different time and size scales. Also, they are quite expensive and not always available, as well as difficult from the point of view of data processing. As well, usually there is only one IL-solvent system under investigation which means that the approach for studying such objects should be wider and more universal. Molecular dynamics (MD) simulation can help solve these problems, and this method can also complete the picture with information not available from experiment .

In this work MD simulation of twelve mixtures of ILs (1-butyl-3-methylimdazolium (C_4mim^+) with tetrafluoroborate (BF_4^-), hexafluorophosphate (PF_6^-), trifluoromethanesulfonate (TFO^-) and bis(trifluoromethane)sulfonimide ($TFSI^-$)) with molecular solvents (acetonitrile (AN), propylene carbonate (PC) or gamma butyrolactone (γ-BL)) of six IL mole fractions were performed. The molecular structures of the objects are presented at Figure 1. The microstructure, clusterization and, finally, the transport properties of the systems have been studied.

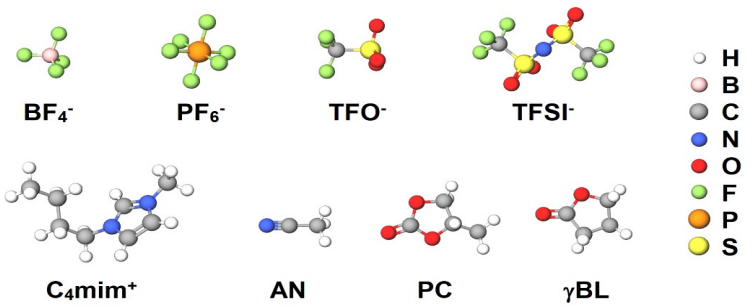

Figure 1. Structure of the ions and molecular solvents considered in this study

Methodology

Details of molecular dynamics simulation. MD simulations have been performed at the temperature of 298.15 K. To set the size of the cubic simulation box, a short (i.e., 1 ns) run has been performed on the isothermal-isobaric *NPT* ensemble at 1 bar. All simulations have been carried out using the GROMACS 2019.4 software package . The temperature and the pressure have been kept constant by means of the velocity-rescaling thermostat with the relaxation time of 0.1 ps, and the Berendsen barostat with the relaxation time of 0.5 ps, respectively. Equations of motion have been integrated using the leap-frog algorithm with a time-step of 0.5 fs. All interactions have been truncated to zero beyond the center-center cut-off distance of 1.2 nm. The long-range part of the electrostatic interaction has been accounted for by the particle mesh Ewald method , while that of the Lennard-Jones interaction has been treated by the conventional shifted force technique. The Lennard-Jones parameters corresponding to unlike pairs of atoms have been calculated by the standard Lorentz-Berthelot combination rules . After equilibrating the systems in the *NPT* ensemble, simulations of 10 ns have been performed in the *NVT* ensemble using the equilibrium density obtained from the constant pressure run. Each set of systems was simulated five times, starting from independently generated random configurations. These parallel calculations were then used to average the data for all structural and transport properties. The last 1 ns of the trajectories from these simulations were used for detailed structural analyses, while the full 10 ns trajectories were utilized for calculating transport properties.

The simulations of the binary mixtures (total of twelve systems) of four ILs of C_4mim^+ cation with different anions (BF_4^-, PF_6^-, TFO^- and $TFSI^-$) in three aprotic dipolar molecular solvents (AN, PC and γ-BL) have been performed. Six different compositions of the mole fraction of the ILs from 0.05 to 0.30 for each binary mixture were selected in a way that the total number of ion pairs for each composition was always equal to 100. The number of the different particles of the ILs in the simulated systems are collected in Table 1.

Table 1. Composition of the systems simulated.

IL mole fraction	Number of cations	Number of anions	Number of solvent molecules
0.05	100	100	1900
0.10			900
0.15			566
0.20			400
0.25			300
0.30			232

The ILs have been described by the potential model of Mondal and Balasubramanian [38-39], while for the solvent molecules the potential model of Koverga et al. [40-41] has been used. According to classical MD formalism, these potential models have the following functional form of the total potential energy:

$$U_{tot} = \sum_{ij}^{bonds} \frac{k_{r,ij}}{2}\left(r_{ij} - r_{0,ij}\right)^2 + \sum_{ijk}^{angles} \frac{k_{\theta,ijk}}{2}\left(\theta_{ijk} - \theta_{0,ijk}\right)^2 + \sum_{ijkl}^{dihedral} \sum_{n=0}^{5} C_n \left(\cos\left(\psi_{ijkl}\right)\right)^n + \\ + \sum_{ij}^{nonbonded} \left(4\varepsilon_{ij} \left[\left(\frac{\sigma_{ij}}{r_{ij}}\right)^{12} - \left(\frac{\sigma_{ij}}{r_{ij}}\right)^{6} \right] + \frac{q_i q_j}{4\pi\varepsilon_0 r_{ij}} \right), \quad (1)$$

where k is the force constant for bond stretching (r), angle bending (θ), torsion (ϕ), respectively, ε and σ are the Lennard-Jones energy and the distance parameters, respectively, and q stands for the fractional charges of the interaction sites. For torsion angle $\psi_{ijkl} = 180^o - \phi_{ijkl}$. Indices i, j, k and l run through the interaction sites of the particles, while the subscript '0' refers to the equilibrium value of the bond lengths and angles. The potential model of ILs can be regarded a refinement of the CLaP force field [42-44]. Thus, while the bond and angle parameters have been retained, the torsional

parameters have been adapted to the Ryckaert-Bellemans analytical expression . Further, the charge distribution of the ions has been optimized in order to improve the agreement with the experimental thermodynamic and transport properties of the studied ILs. Thus, the ions of the IL carry a net charge that depends on the anion [38-39]. The potential models used here were previously validated by their ability of reproducing the basic experimental physicochemical properties of the systems [38-39].

Aggregate analysis. To study the association of ions, it is essential to establish a criterion by which two ions can be considered part of the same aggregate, cluster, or associate. Such a criterion was proposed in different works [46-47] as the distance between coordination centers of respective ions. Thus, two ions were considered to belong to the same associate if their respective centers are located at the equal or lower distance that was chosen as a criterion from each other .

After the definition of the criterion, the neighbor list of each cation and anion was determined for each configuration during the simulation at each timestep. The obtained neighbor list was later used to establish the connectivity between ions in the system. Important to note that mainly differently charged ions are coordinating around each other (anions around cations and vice versa). This means that the resulting clusters are constructed from the ions of altering charge that have the distance between them that fulfill the determined criterion.

Finally, the statistical analysis was applied to determine the characteristics of clusters. One of such statistical functions can be a size distribution of the aggregates $P(n)$. It shows the probability of finding an ion in an aggregate of size n:

$$P(n) = \frac{n\sum_{j=1}^{C} A_n(j)}{CN}, \tag{2}$$

where $A_n(j)$ is the number of aggregates of size n for a given configuration j, C is the total number of configurations acquired during the simulation, N is the total number of cations and anions combined in the simulation box.

To better represent the results of the clusterization the average number of association $\overline{n}$ can be obtained. In general case, one can calculate it as follows:

$$\overline{n} = \sum_{i=1}^{N} n_i P_i(n) \tag{3}$$

Aggregate analysis has been performed by AGGREGATES 3.2.0 software package .

Transport properties. The coefficient of translational self-diffusion of atoms (molecules, ions) in a liquid can be found using the Green-Kubo relation:

$$D = \frac{1}{3}\int_0^{\infty} C_{vv}(t)\,dt. \tag{4}$$

For the viscosity a nonequilibrium periodic perturbation method has been used . To sum it up, molecular dynamic simulation is carried out in the 3D periodic cell with the external force in x direction $a(z)$. According to the Navier-Stokes's equation:

$$\rho\frac{\partial u}{\partial t} + \rho(u\cdot\nabla)u = \rho a - \nabla p + \eta\nabla^2 u, \tag{5}$$

where u is the velocity of the liquid, p is pressure of the fluid, ρ is the density of the fluid, t is time, η is viscosity. Because force is applied only in the x direction, the velocity along y and z will be zero:

$$\rho\frac{\partial u_x(z)}{\partial t} = \rho a_x(z) + \eta\frac{\partial^2 u_x(z)}{\partial z^2}. \tag{6}$$

The velocity profile as well as acceleration should be periodic because of the periodic system in the simulations. Thus, the cosine function can be used for this purpose:

$$a_x(z) = \Lambda\cos(kz), \tag{7}$$

$$k = \frac{2\pi}{l_z}, \tag{8}$$

where l_z is the height of the box, Λ is the acceleration amplitude of the external force. The viscosity then can be obtained:

$$\eta = \frac{\Lambda}{V}\frac{\rho}{k^2}. \tag{9}$$

The measured viscosity greatly depends on the parameter Λ. To obtain the viscosity at zero acceleration few viscosities for different accelerations should be obtained. Then plotting the viscosities versus the amplitudes allows to obtain shear viscosity for Λ=0 via extrapolation.

Results and discussion

Structural properties. With the aim to study the cation-anion interaction, the interionic radial distribution functions (RDFs) and running coordination numbers (RCNs) of IL-solvent binary mixtures were analyzed. To fully consider these interactions the respective atoms for cations and anions should be chosen. Also, these points in space need to take into consideration all the coordination centers of cations and anions at once. For the C_4mim^+ , the most positive charge is localized at the hydrogen sites around the imidazolium ring. Given this fact the center of the ring (CoR) is usually chosen as a reference point for the analysis [51-53]. Due to different structure, shape and symmetry of the anions their positions (X) for the analysis will be the follows: B atom in BF_4^-, P atom in PF_6^-, middle of the C-S bond in TFO^- (takes into account both O and F coordination sites) and N atom in $TFSI^-$ (takes into account N, O and F coordination sites).

The interionic RDFs for all IL-solvent binary mixtures for all simulated systems are shown in Figure 2.

Here the similar curves were obtained for all IL mole fractions, meaning the positions of the peaks and minima do not depend on the concentration of the IL. Furthermore, their positions do not vary at all for the same IL in different solvents. The first maxima for various anions occur at 0.49 nm (BF_4^-), 0.51 nm (PF_6^-) and 0.52 nm (TFO^-). For the $TFSI^-$ anion the situation is more complicated as there are two peaks at relatively low distances, 0.44 nm and 0.62 nm respectively. Also, these peaks have lower intensity comparing to other ILs. The first maximum in this case corresponds to the CoR-N interaction when N atom is located directly near the center of the ring or the H-atoms of the ring (the distances in both cases are similar). At the same time the second peak indicates the CoR-N interaction when N atom of $TFSI^-$ not directly interacting with the ring, but instead the oxygen atoms do. The example snapshot from the MD simulation trajectory files was obtained via VMD program package (Figure 3). These findings prove the quantum chemical calculations from the literature data . The first minima of RDFs for various anions are as follows: 0.70 nm (BF_4^-), 0.74 nm (PF_6^-), 0.73 nm (TFO^-) and 0.77 nm ($TFSI^-$). The behavior of the intensities of the peaks also changes in different ILs-solvent combinations. For all systems with AN the intensity becomes lower with the increasing of the ILs mole fraction. Also, for $TFSI^-$ system these changes are the lowest. Similar situation can be observed for all PC-containing systems where peak intensity do not change with the mole fraction of the ILs.

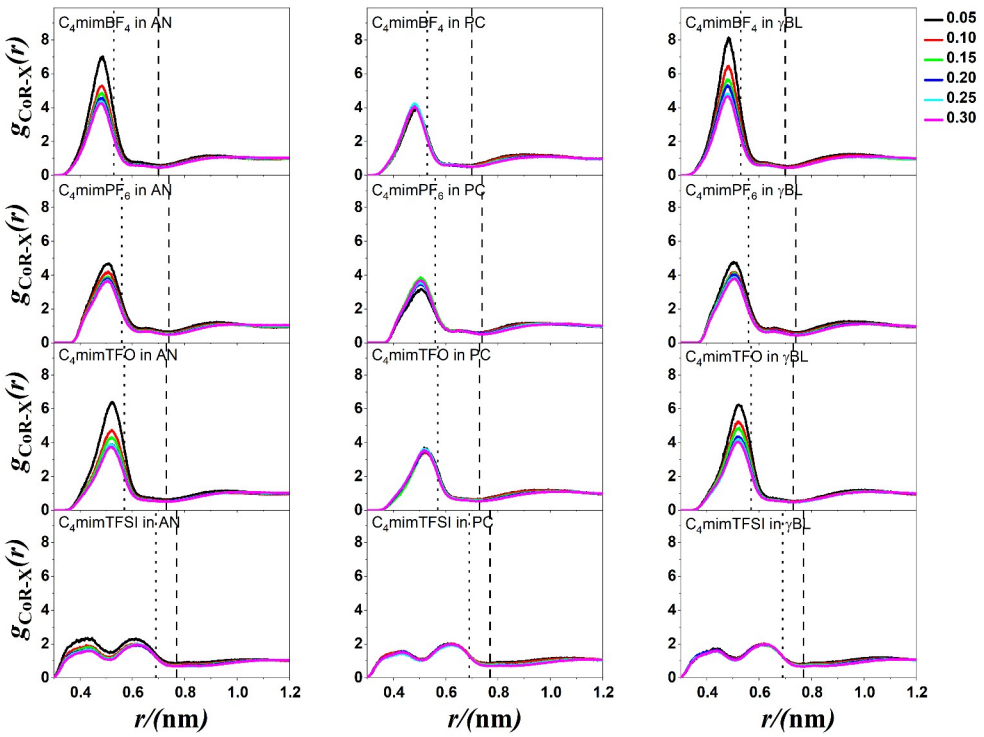

Figure 2. Cation-anion (CoR-X) radial distribution functions of the mixtures at various mole fraction of ionic liquid. The position of the cation is described with center of imidazolium ring. The positions of anions (X) are: B atom in BF_4^-, P atom in PF_6^-, middle of the C-S bond in TFO^- and N atom in $TFSI^-$. The vertical dashed and dotted lines correspond to the first and criterion, respectively, for aggregation analysis.

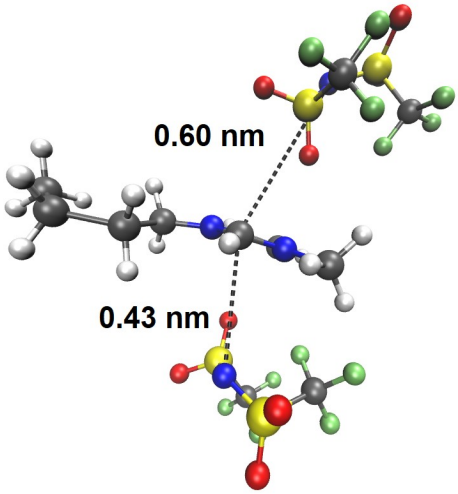

Figure 3. Example of $(C_4mim(TFSI)_2)^-$ associate in one of the C_4mimTFSI system

The RCNs between cations and anions for all IL-solvent binary mixtures for all the systems simulated are presented in Figure 4.

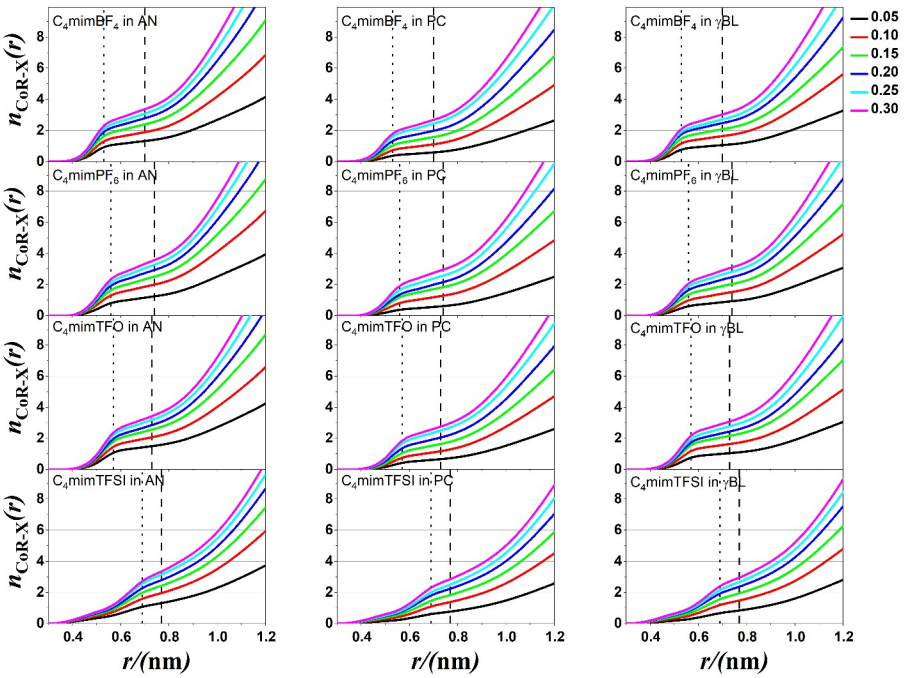

Figure 4. Cation-anion (CoR-X) running coordination numbers of the mixtures at various mole fraction of ionic liquid. The position of the cation is described with center of imidazolium ring. The positions of anions (X) are: B atom in BF_4^-, P atom in PF_6^-, middle of the C-S bond in TFO^- and N atom in $TFSI^-$. The vertical dashed and dotted lines correspond to the first and second criteria respectively, used for aggregation analysis.

The expected increase of the coordination number of the anion around the cation with the IL mole fraction increase can be observed at all of the graphs. The values of the coordination numbers however depend on the solvent. E.g., for AN it varies from ~1.2 (0.05 mole fraction of IL) to ~3.6 (0.30 mole fraction of IL), for PC – from 0.6 to 3.0 and for γ-BL – from 0.8 to 3.1 for all ILs. The coordination numbers of AN system being the biggest indicate the lowest among other solvent molecules dipole moment and as a result the weakest ion-solvent interaction in these systems, meaning with the ILs fraction increase the AN molecules are actively replaced with the anions in the cation first coordination sphere. Also, in the case of all $TFSI^-$ systems the curves values do not increase until at bigger distances.

Aggregate analysis. The ionic aggregates existence was analyzed via two different criteria. First criterion is the first minimum on the cation-anion RDF (Figure 2). This distance shows the border for the first coordination sphere where all of the anions are in strong interaction with the C_4mim^+ cation. As a second criterion the minimum on the second derivative of the RCN curve was proposed (Figure 5).

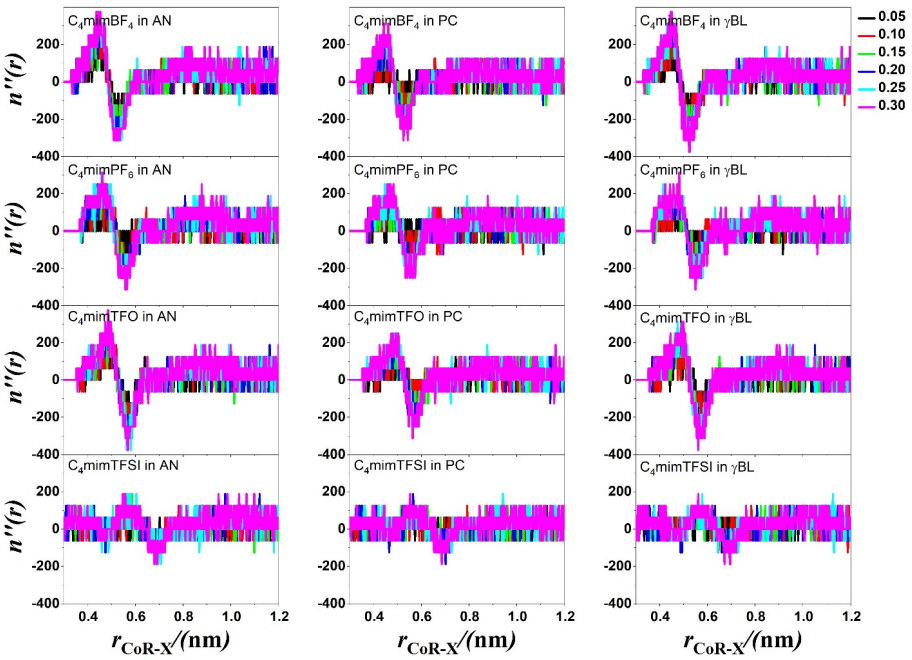

Figure 5. Second derivatives of the cation-anion (CoR-X) running coordination numbers of the mixtures at various mole fraction of ionic liquid. The position of the cation is described with center of imidazolium ring. The positions of anions are: B atom in BF_4^-, P atom in PF_6^-, middle of the C-S bond in TFO^- and N atom in $TFSI^-$.

This minimum marks the point where the RCN curve transitions to a plateau following an initial rapid increase. It is slightly shifted from the first peak in the RDF, or the second peak in systems containing the $TFSI^-$ anion, as explained in the previous section. The values of the distances for this criterion are next: 0.53 nm (BF_4^-), 0.56 nm (PF_6^-), 0.57 nm (TFO^-) and 0.69 nm ($TFSI^-$).

The results of the clusters formation probability for all mixtures of all mole fractions can be found in Figures 6-17 for the first and second criteria respectively.

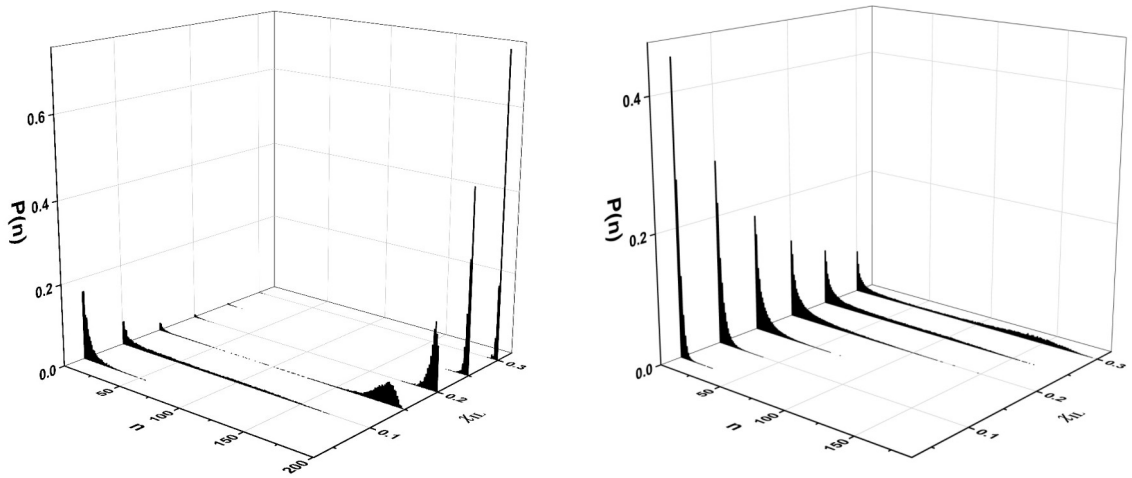

Figure 6. Probability distributions of aggregate sizes with first (left) and second (right) criterion of the C_4mimBF_4 in AN binary mixture at various mole fraction of ionic liquid.

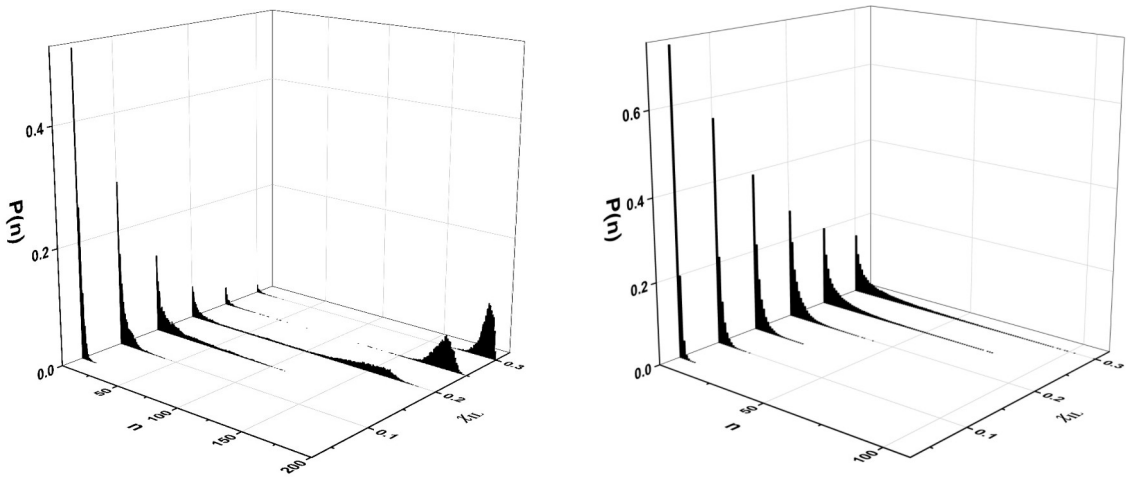

Figure 7. Probability distributions of aggregate sizes with first (left) and second (right) criterion of the C_4mimBF_4 in PC binary mixture at various mole fraction of ionic liquid.

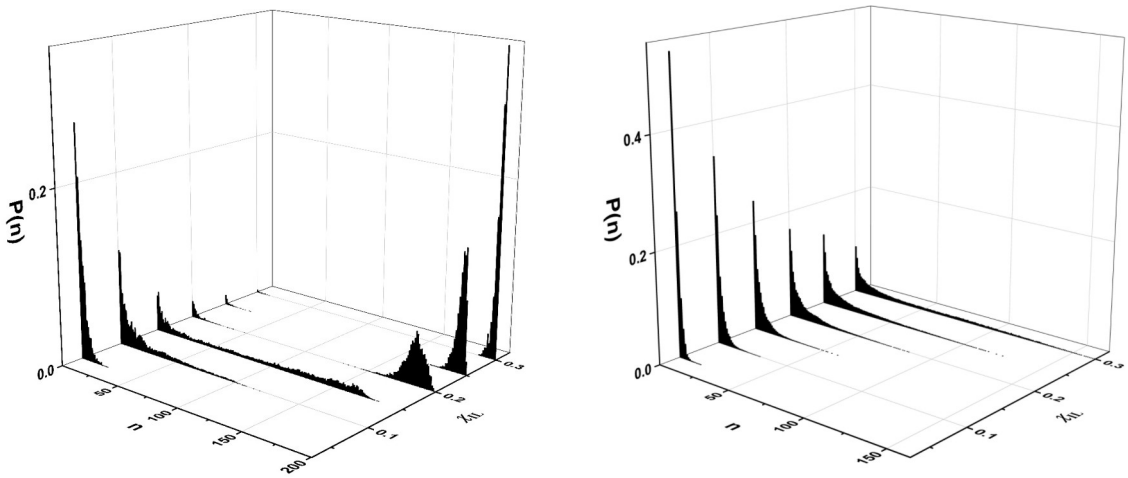

Figure 8. Probability distributions of aggregate sizes with first (left) and second (right) criterion of the C_4mimBF_4 in γ-BL binary mixture at various mole fraction of ionic liquid.

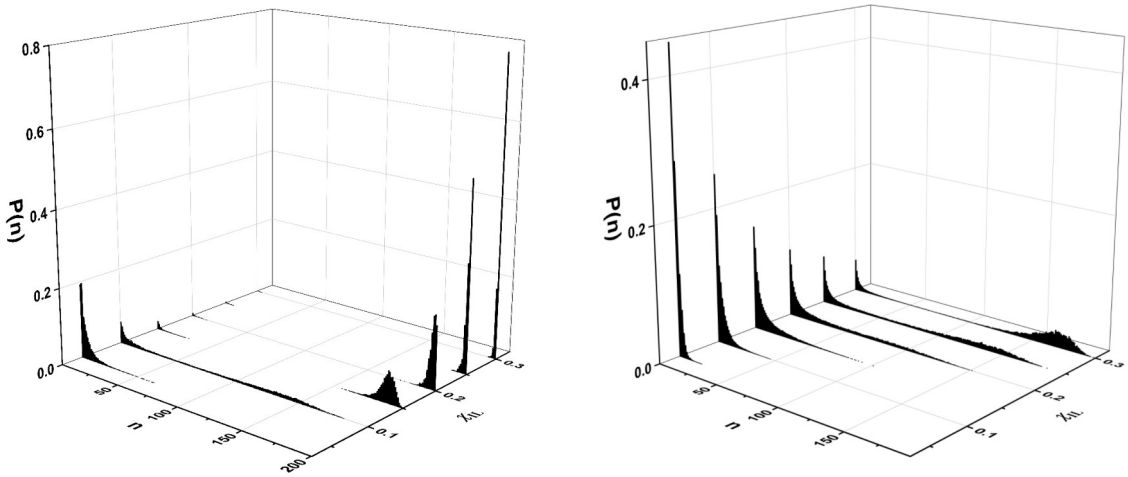

Figure 9. Probability distributions of aggregate sizes with first (left) and second (right) criterion of the C_4mimPF_6 in AN binary mixture at various mole fraction of ionic liquid.

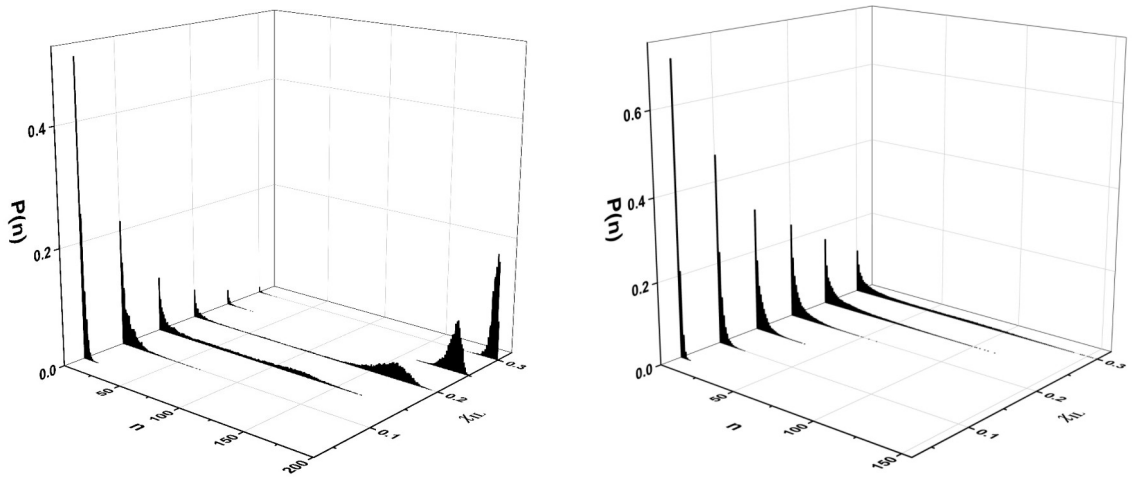

Figure 10. Probability distributions of aggregate sizes with first (left) and second (right) criterion of the C_4mimPF_6 in PC binary mixture at various mole fraction of ionic liquid.

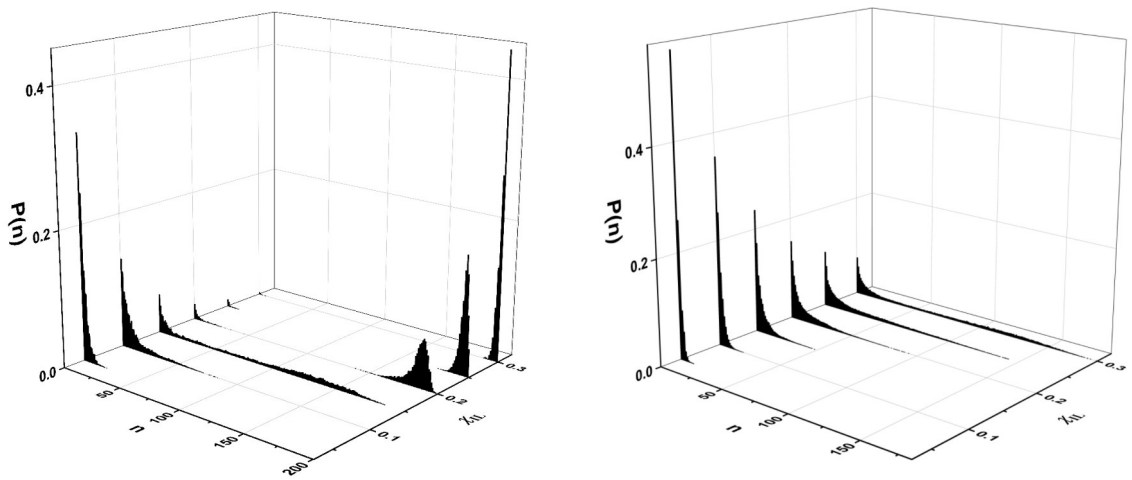

Figure 11. Probability distributions of aggregate sizes with first (left) and second (right) criterion of the C_4mimPF_6 in γ-BL binary mixture at various mole fraction of ionic liquid.

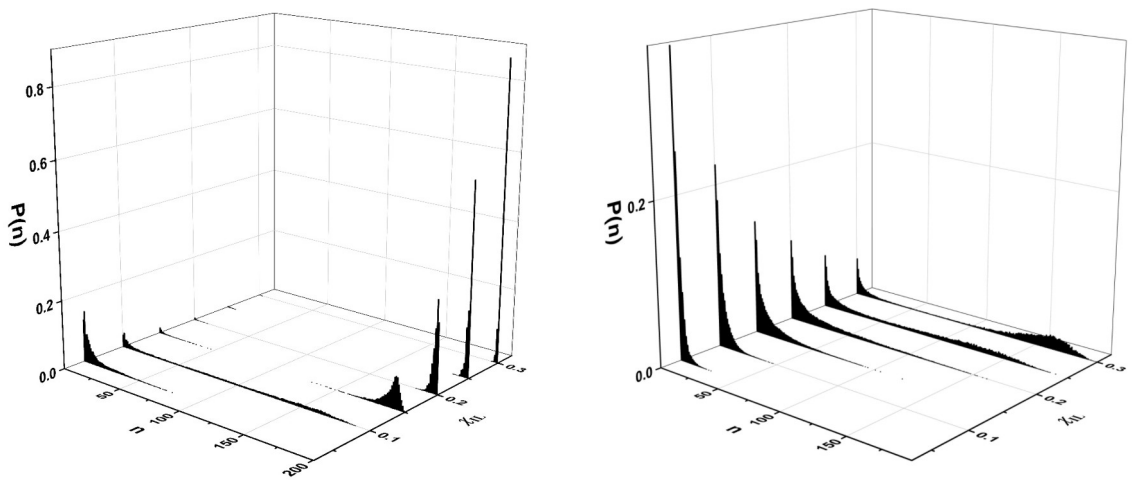

Figure 12. Probability distributions of aggregate sizes with first (left) and second (right) criterion of the $C_4mimTFO$ in AN binary mixture at various mole fraction of ionic liquid.

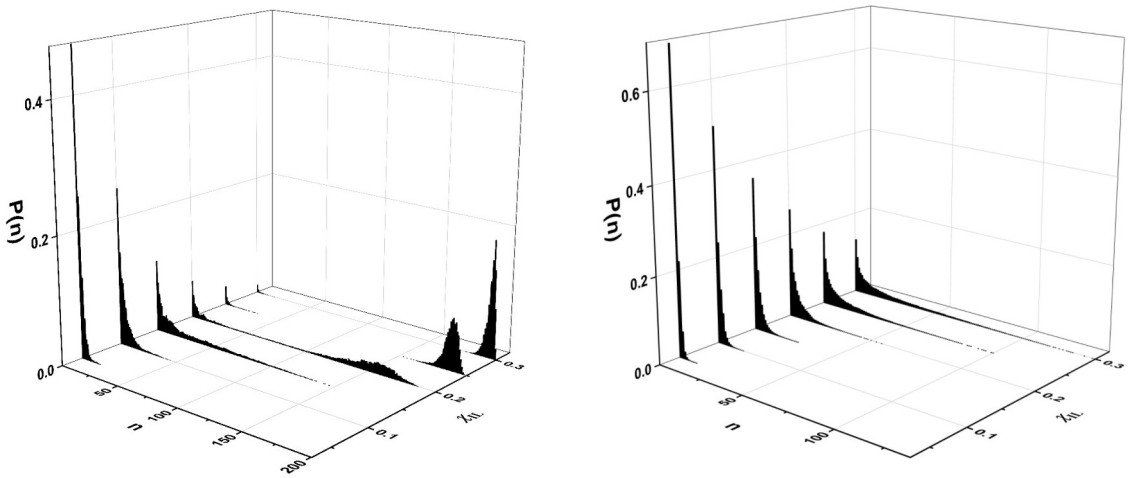

Figure 13. Probability distributions of aggregate sizes with first (left) and second (right) criterion of the C_4mimTFO in PC binary mixture at various mole fraction of ionic liquid.

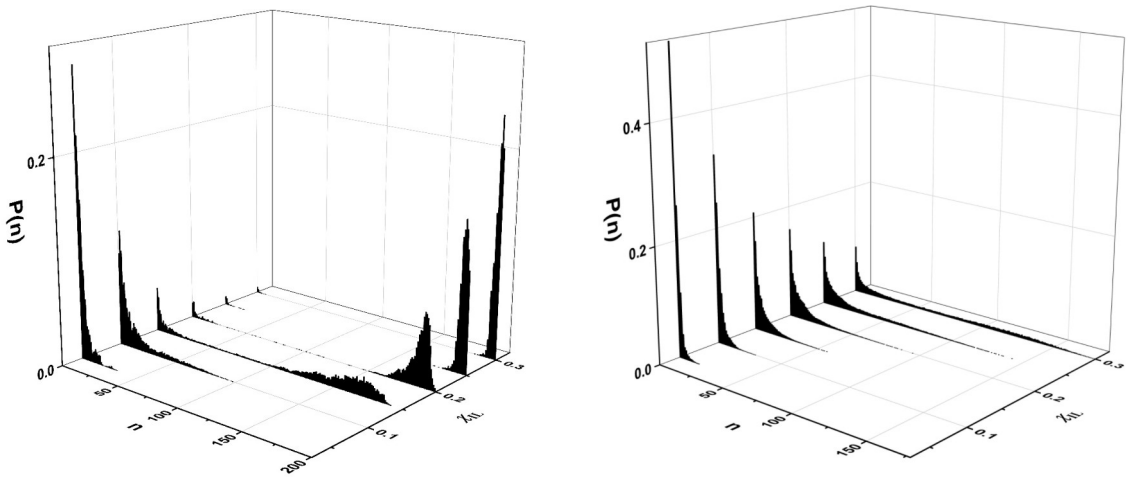

Figure 14. Probability distributions of aggregate sizes with first (left) and second (right) criterion of the C_4mimTFO in γ-BL binary mixture at various mole fraction of ionic liquid.

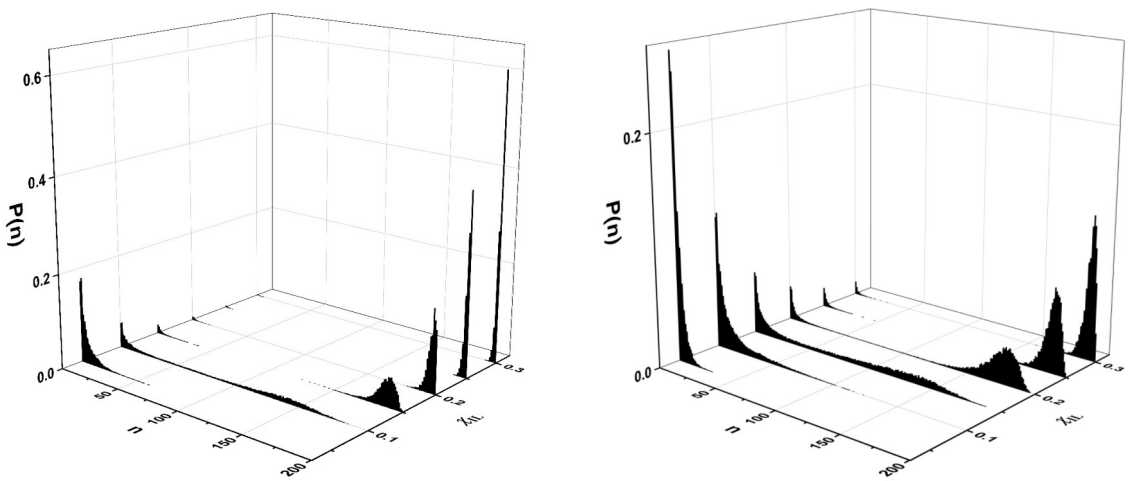

Figure 15. Probability distributions of aggregate sizes with first (left) and second (right) criterion of the C_4mimTFSI in AN binary mixture at various mole fraction of ionic liquid.

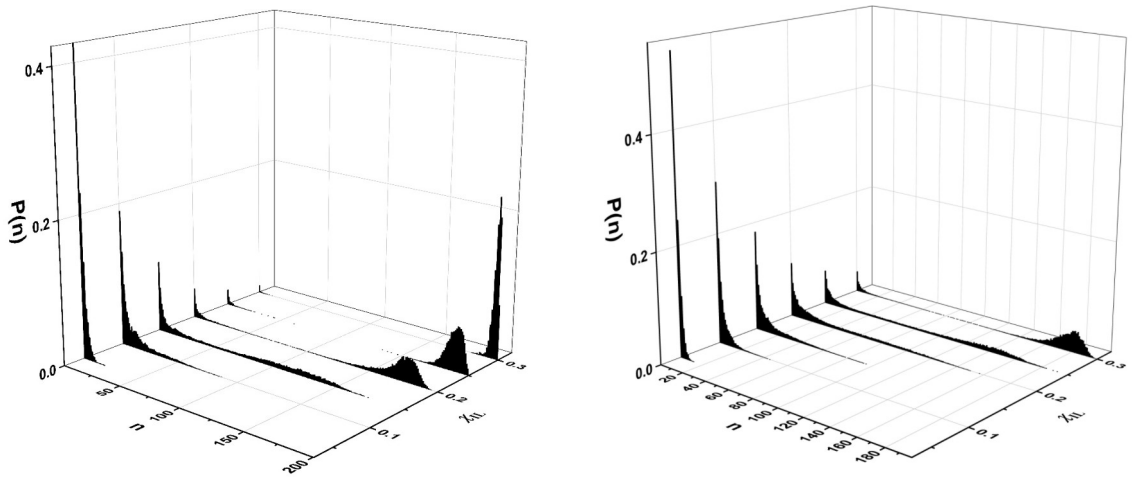

Figure 16. Probability distributions of aggregate sizes with first (left) and second (right) criterion of the C_4mimTFSI in PC binary mixture at various mole fraction of ionic liquid.

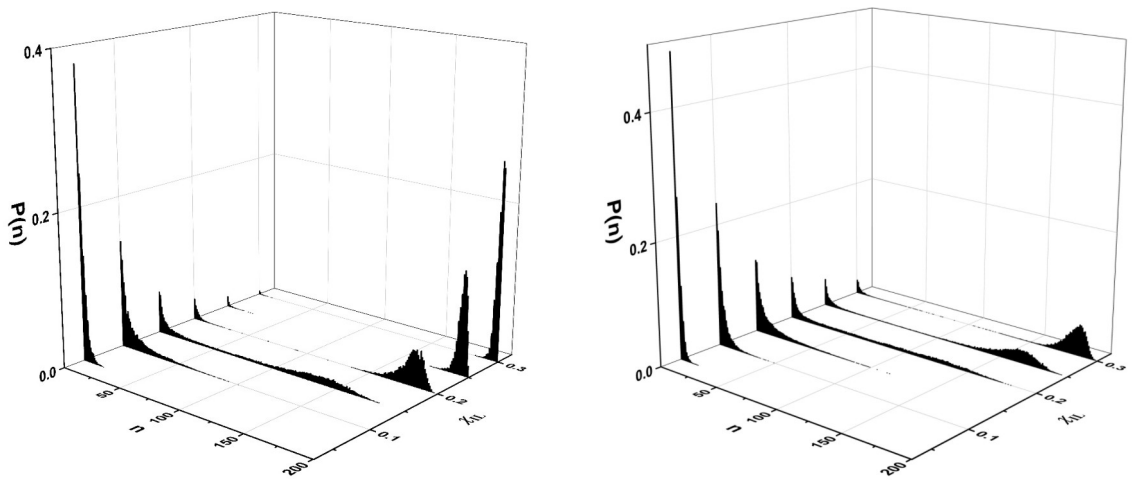

Figure 17. Probability distributions of aggregate sizes with first (left) and second (right) criterion of the C_4mimTFSI in γ-BL binary mixture at various mole fraction of ionic liquid.

The aggregates increase in size with the increasing of the IL mole fraction for each system. The small clusters are dominating in the most diluted systems when using the first criteria. As the mole fraction of IL increases up to 0.10 for AN mixtures, 0.15 for PC mixtures, and 0.20 for γ-BL mixtures, transition systems are formed in which a large number of aggregates of different types are present. With the further increase of mole fraction of the ILs all the systems start to form large aggregates that include most of the ions in the mixture can be observed. The existence of such huge continuous polar network, however, still allows small clusters or even isolated ions to exist in systems. Most probably these small aggregates lose the connectivity with the huge cluster, but their low probabilities of formation prove that it is a temporary phenomenon. At the highest observed concentration, nevertheless, the ions are part of one massive associate.

It shows that at the first distance criterion (minimum on the interionic RDF) the aggregate formation is overestimated in the mixture as there are no charge carriers left in this case and thus there should be no conductivity at these mole fraction of the ILs. However, the experimental results show otherwise [55-58].

As for the second criteria, it shows that transition to the massive association occurs only at the highest IL mole fraction of 0.30 (for $TFSI^-$ – at 0.20-0.25). However, for the binary mixtures with AN the tendency for larger clusters formation appears at lower IL mole fraction compared to PC and γ-BL mixtures. This shows that AN demonstrates a weaker ion-solvent interaction, allowing ions at lower concentration form a continuous polar network regardless of the chosen criteria.

To better illustrate the clusterization processes the average numbers of associations were obtained for all systems (Figure 18). The figure displays in more compact way the same results that were discussed earlier. Here for the first criterion ions in AN systems form massive aggregates at 0.15 mole fraction of ILs already, in γ-BL and PC mixtures – at 0.20 and 0.25 respectively. For the second criterion the ions in the systems are separated from each other or forming small aggregates until ~0.15-0.20 mole fraction of the ILs. After that value of mole fraction ILs in mixtures tend to form bigger aggregates. For the BF_4^-, PF_6^- and TFO^- in PC this trend is not so pronounced. The massive aggregation process occurs only in $TFSI^-$ systems for the second criterion and only at highest concentration of 0.30. The AN systems at this concentration at the transition stage, however for the C_4mimTFSI in AN mixture almost all ions are part of the big associate even at the mole fraction of ILs of 0.25.

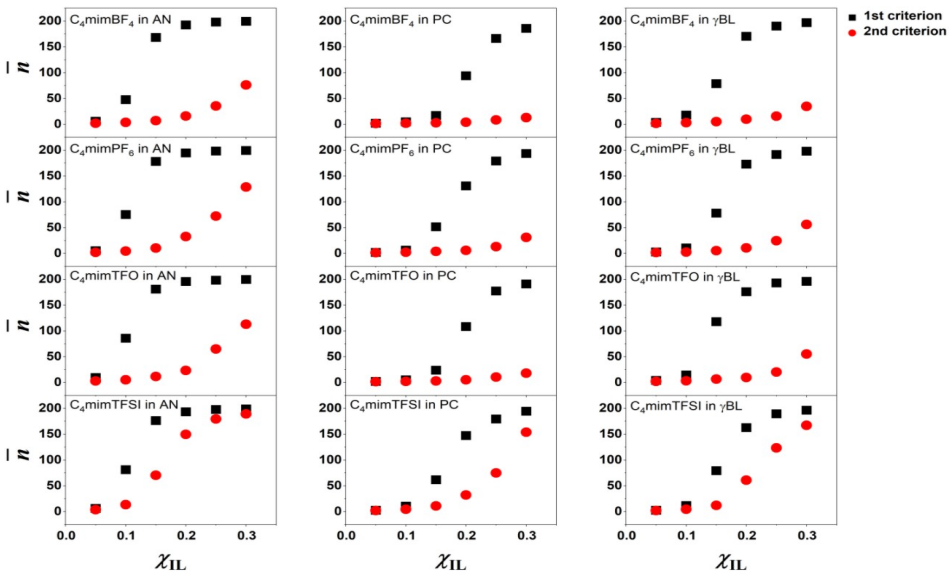

Figure 18. Average numbers of association with first minima on the RDFs (1st criteria) and with the minima on the second derivative on the RCN (2nd criteria) of the mixtures at various mole fraction of ionic liquid.

Nernst-Einstein relation postulates that conductivity depends on the concentration of the charge carriers in the solution :

$$\kappa = \frac{e^2}{Vk_BT}\left(N_+ z_+^2 \overline{D}_+ + N_- z_-^2 \overline{D}_-\right) \tag{10}$$

where e is the elementary charge, k_B – Boltzmann constant, V – volume of the system, T – temperature of the system, $z_\pm$ – charge of the ion, $N_\pm$ – number of cations and anions.

Ionic aggregation reduces its concentration and effectively causes the drop in the conductivity value. As seen from the Figure 18, the mole fractions of rapid increase in the aggregates formation are the same as the conductivity maxima are located: at ~0.10 for AN systems and at ~0.20 for PC and γ-BL ones [55-58].

Transport properties. The diffusion coefficients and shear viscosities were obtained for all the IL mole fractions for all systems. The results are presented at Figures 19 and 20 respectively.

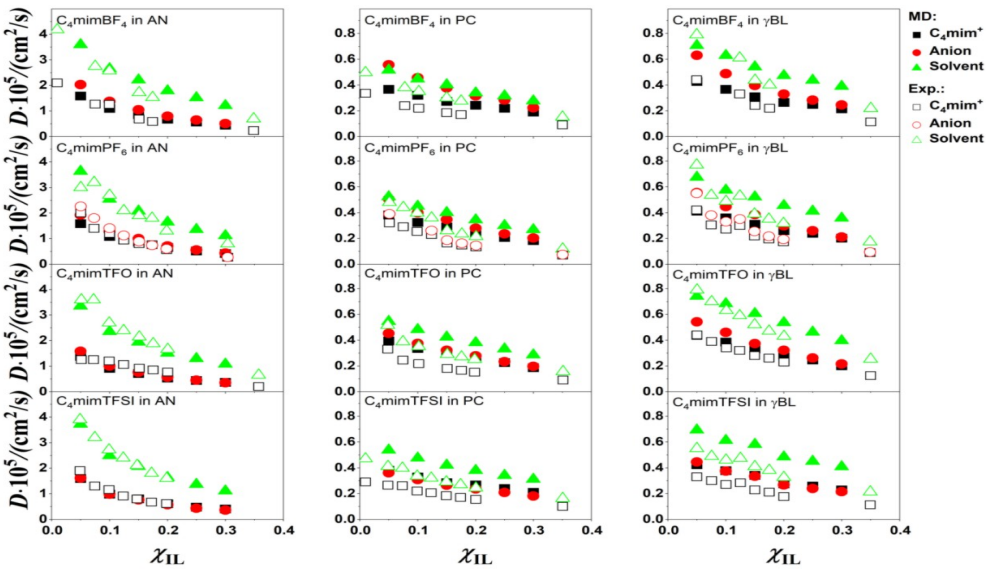

Figure 19. Diffusion coefficients for cation, anions and solvent molecules in comparison with the experimental data of the mixtures at various mole fraction of ionic liquid.

The diffusion coefficients were compared to the experimental data for cations and solvent molecules (and also for anions for the systems with PF_6^-) . For the binary mixtures with AN the obtained coefficients are very close to the experimental ones for all of the components of the analysis. For the systems with PC and γ-BL the obtained diffusion coefficients have in general higher values comparing to the experiment by 20%, especially for the higher concentrations.

For all systems the diffusion coefficients of the solvent molecules are higher than of the cation or anions, while the latter are close to each other for almost all systems and IL mole fractions. Also, the coefficients of the components in the systems with AN molecules are 3-5 times higher than with other two solvent molecules. For all PC systems the general trend is almost similar diffusion coefficient for anion and solvent molecule. For the C_4mimBF_4 in PC simulated system the anion diffusion coefficient is even higher in the most diluted solution. On the other hand, this behavior cannot be observed in the experimental data.

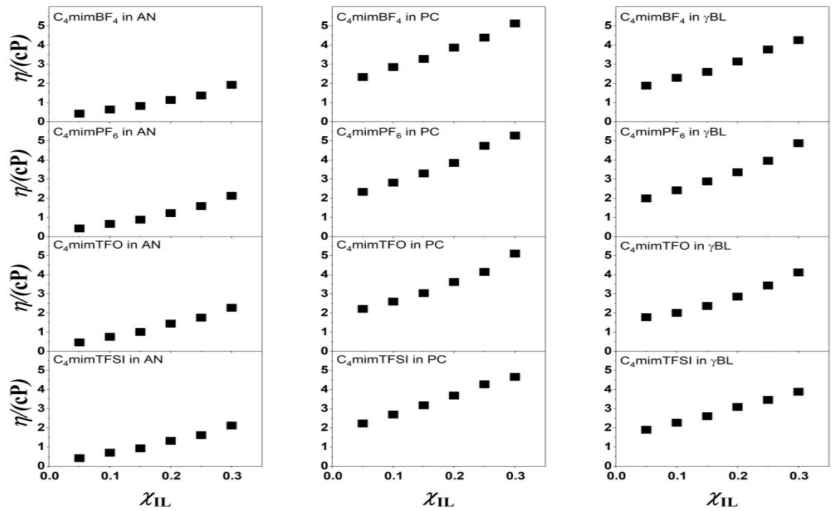

Figure 20. Viscosities of the mixtures at various mole fraction of ionic liquid

The viscosities at Figure 20 are increasing with the IL mole fraction increase by a non-linear dependance. Although, the values for all systems do not show any drastic changes at respective mole fractions where the experimental conductivity has maximum.

As the Nernst-Einstein relation shows (Equation 10), not only concentration of the charge carriers influence the conductivity but the diffusion coefficients as well . The behavior of calculated diffusion coefficients from the simulation for ions is in agreement with this statement.

Conclusions

In current work twelve ILs (C_4mim^+ with BF_4^-, PF_6^-, TFO^- and $TFSI^-$) with molecular solvents (acetonitrile, propylene carbonate, and gamma butyrolactone) binary mixtures were studied by the molecular dynamics simulation technique.

The microstructure of the mixtures was studied in the framework of radial distribution functions and running coordination numbers. The RDFs and RCNs show the particular behavior in AN and $TFSI^-$ systems. For TFSI- system the cation-anion (CoR-N) RDFs curves showed two peaks with similar intensities. It was shown that they represent the position when the nitrogen atom of the anion is close to the imidazolium ring and when nitrogen atom of $TFSI^-$ not directly interacting with the ring, but instead the oxygen atoms do. The cation-anion coordination numbers changed in similar values for the same ionic liquids in different solvents: for AN it varies from ~1.2 to ~3.6, for PC – from 0.6 to 3.0 and for γ-BL – from 0.8 to 3.1 with the increasing mole fraction of the ILs. Also, data obtained were used to conduct a quantitative aggregate analysis with two different distance criteria (first minimum of RDF and minimum of the second derivative of the RCN respectively) to compare the results with each other. The analysis with the first criterion shows the formation of the massive cluster at ~0.15, 0.20 and 0.25 IL mole fraction for AN and for with γ-BL respectively. Thus, this criterion seems to overrate the aggregation process in the mixtures. With the second, shorter distance criterion the formation of big aggregates in the systems starting to occur at the same mole fractions of the ILs where the experimental conductivity curves change their behavior and the maximum occurs. It proves that the reason of such drastic changes in the conductivity particular lies in the local structure of the ILs and solvent molecules.

To evaluate the transport properties, we obtained the diffusion coefficients for all components and the shear viscosity for all binary mixtures. The diffusion coefficients closely align with experimental data, demonstrating excellent accuracy, particularly for systems containing AN. Although the viscosity measurements did not reveal any distinct trends at the mole fraction range of ILs corresponding to the experimental conductivity maximum, these findings provide valuable insights into the complex interactions within these mixtures.

Acknowledgement

D.S.D., Y.V.K. and O.N.K acknowledge the Ministry of Education and Science of Ukraine for the Grant No. 0122U001485. The calculations were performed on the *Dell EMC PowerEdge R740 supercomputer* of the Center for collective use of scientific equipment "*Laboratory of micro- and nano-systems, new materials and technologies*" of the Ministry of Education and Science of Ukraine at V.N. Karazin Kharkiv National University and *Azzurra HPC center*, Université Côte d'Azur, Nice, France.

References

1. Dorbritz S., Ruth W., Kragl U. Investigation on aggregate formation of ionic liquids. *Advanced Synthesis & Catalysis* 2005, *347* (9), 1273-1279. https://doi.org/10.1002/adsc.200404352
2. Andanson J. M., Traïkia M., Husson P. Ionic association and interactions in aqueous methylsulfate alkyl-imidazolium-based ionic liquids. *The Journal of Chemical Thermodynamics* 2014, *77* 214-221. https://doi.org/10.1016/j.jct.2014.01.031
3. Bešter-Rogač M., Stoppa A., Hunger J., Hefter G., Buchner R. Association of ionic liquids in solution: A combined dielectric and conductivity study of [bmim][cl] in water and in acetonitrile. *Physical Chemistry Chemical Physics* 2011, *13* (39), 17588-17588. https://doi.org/10.1039/C1CP21371G
4. Jan R., Rather G. M., Bhat M. A. Association of ionic liquids in solution: Conductivity studies of [bmim][cl] and [bmim][pf6] in binary mixtures of acetonitrile + methanol. *Journal of Solution Chemistry* 2013, *42* (4), 738-745. https://doi.org/10.1007/s10953-013-9999-4
5. Hou J., Zhang Z., Madsen L. A. Cation/anion associations in ionic liquids modulated by hydration and ionic medium. *Journal of Physical Chemistry B* 2011, *115* (16), 4576-4582. https://doi.org/10.1021/jp1110899

6. Boruń A. Conductance and ionic association of selected imidazolium ionic liquids in various solvents: A review. *Journal of Molecular Liquids* 2019, *276* 214-224. https://doi.org/10.1016/j.-molliq.2018.11.140
7. Lovelock K. R. J. Quantifying intermolecular interactions of ionic liquids using cohesive energy densities. *Royal Society Open Science* 2017, *4* (12), 171223-171223. https://doi.org/10.1098/rsos.171223
8. Fumino K., Reimann S., Ludwig R. Probing molecular interaction in ionic liquids by low frequency spectroscopy: Coulomb energy, hydrogen bonding and dispersion forces. *Physical Chemistry Chemical Physics* 2014, *16* (40), 21903-21929. https://doi.org/10.1039/C4CP01476F
9. Anderson J. L., Ding J., Welton T., Armstrong D. W. Characterizing ionic liquids on the basis of multiple solvation interactions. *Journal of the American Chemical Society* 2002, *124* (47), 14247-14254. https://doi.org/10.1021/ja028156h
10. Angenendt K., Johansson P. Ionic liquid structures from large density functional theory calculations using mindless configurations. *The Journal of Physical Chemistry C* 2010, *114* (48), 20577-20582. https://doi.org/10.1021/jp104961r
11. Xiong Z., Gao J., Zhang D., Liu C. Hydrogen bond network of 1-alkyl-3-methylimidazolium ionic liquids: A network theory analysis. *Journal of Theoretical and Computational Chemistry* 2012, *11* (3), 587-598. https://doi.org/10.1142/S0219633612500381
12. Niemann T., Strate A., Ludwig R., Zeng H. J., Menges F. S., Johnson M. A. Cooperatively enhanced hydrogen bonds in ionic liquids: Closing the loop with molecular mimics of hydroxy-functionalized cations. *Physical Chemistry Chemical Physics* 2019, *21* (33), 18092-18098. https://doi.org/10.1039/C9CP03300A
13. Le Donne A., Adenusi H., Porcelli F., Bodo E. Hydrogen bonding as a clustering agent in protic ionic liquids: Like-charge vs opposite-charge dimer formation. *ACS Omega* 2018, *3* (9), 10589-10600. https://doi.org/10.1021/acsomega.8b01615
14. Fumino K., Wulf A., Ludwig R. Hydrogen bonding in protic ionic liquids: Reminiscent of water. *Angewandte Chemie International Edition* 2009, *48* (17), 3184-3186. https://doi.org/10.1002/anie.200806224
15. Brela M. Z., Kubisiak P., Eilmes A. Understanding the structure of the hydrogen bond network and its influence on vibrational spectra in a prototypical aprotic ionic liquid. *Journal of Physical Chemistry B* 2018, *122* (41), 9527-9537. https://doi.org/10.1021/acs.jpcb.8b05839
16. Avent A. G., Chaloner P. A., Day M. P., Seddon K. R., Welton T. Evidence for hydrogen bonding in solutions of 1-ethyl-3-methylimidazolium halides, and its implications for room-temperature halogenoaluminate(iii) ionic liquids. *Journal of the Chemical Society, Dalton Transactions* 1994, (23), 3405-3405. https://doi.org/10.1039/DT9940003405
17. Marekha B. A., Kalugin O. N., Bria M., Idrissi A. Probing structural patterns of ion association and solvation in mixtures of imidazolium ionic liquids with acetonitrile by means of relative ^{1}h and ^{13}c nmr chemical shifts. *Physical Chemistry Chemical Physics* 2015, *17* (35), 23183-23194. https://doi.org/10.1039/C5CP02748A
18. Bester-Rogac M., Stoppa A., Buchner R. Ion association of imidazolium ionic liquids in acetonitrile. *J Phys Chem B* 2014, *118* (5), 1426-35. https://doi.org/10.1021/jp412344a
19. Yalcin D., Drummond C. J., Greaves T. L. Solvation properties of protic ionic liquids and molecular solvents. *Physical Chemistry Chemical Physics* 2019, *22* (1), 114-128. https://doi.org/10.1039/C9CP05711K
20. Sadeghi R., Ebrahimi N. Ionic association and solvation of the ionic liquid 1-hexyl-3- methylimidazolium chloride in molecular solvents revealed by vapor pressure osmometry, conductometry, volumetry, and acoustic measurements. *Journal of Physical Chemistry B* 2011, *115* (45), 13227-13240. https://doi.org/10.1021/jp2055188
21. Dupont J. On the solid, liquid and solution structural organization of imidazolium ionic liquids. *Journal of the Brazilian Chemical Society* 2004, *15* (3), 341-350. https://doi.org/10.1590/S0103-50532004000300002
22. Zhao Y., Gao S., Wang J., Tang J. Aggregation of ionic liquids [cnmim]br (n = 4, 6, 8, 10, 12) in d2o: A nmr study. *Journal of Physical Chemistry B* 2008, *112* (7), 2031-2039. https://doi.org/10.1021/jp076467e

23. Tokuda H., Baek S. J., Watanabe M. Room-temperature ionic liquid-organic solvent mixtures: Conductivity and ionic association. *Electrochemistry* 2005, *73* (8), 620-622. https://doi.org/10.5796/electrochemistry.73.620
24. Richardson P. M., Voice A. M., Ward I. M. Pulsed-field gradient nmr self diffusion and ionic conductivity measurements for liquid electrolytes containing libf4 and propylene carbonate. *Electrochimica Acta* 2014, *130* 606-618. https://doi.org/10.1016/j.electacta.2014.03.072
25. Burrell G. L., Burgar I. M., Gong Q., Dunlop N. F., Separovic F. Nmr relaxation and self-diffusion study at high and low magnetic fields of ionic association in protic ionic liquids. *Journal of Physical Chemistry B* 2010, *114* (35), 11436-11443. https://doi.org/10.1021/jp105087n
26. Kundu K., Chandra G. K., Umapathy S., Kiefer J. Spectroscopic and computational insights into the ion-solvent interactions in hydrated aprotic and protic ionic liquids. *Physical Chemistry Chemical Physics* 2019, *21* (37), 20791-20804. https://doi.org/10.1039/C9CP03670A
27. Danten Y., Cabaço M. I., Besnard M. Interaction of water diluted in 1-butyl-3-methyl imidazolium ionic liquids by vibrational spectroscopy modeling. *Journal of Molecular Liquids* 2010, *153* (1), 57-66. https://doi.org/10.1016/j.molliq.2009.07.001
28. Marcus Y., Hefter G. Ion pairing. *Chemical Reviews* 2006, *106* (11), 4585-4621. https://doi.org/10.1021/cr040087x
29. Shimomura T., Takamuku T., Yamaguchi T. Clusters of imidazolium-based ionic liquid in benzene solutions. *The Journal of Physical Chemistry B* 2011, *115* (26), 8518-8527. https://doi.org/10.1021/jp203422z
30. Russina O., Sferrazza A., Caminiti R., Triolo A. Amphiphile meets amphiphile: Beyond the polar–apolar dualism in ionic liquid/alcohol mixtures. *The Journal of Physical Chemistry Letters* 2014, *5* (10), 1738-1742. https://doi.org/10.1021/jz500743v
31. Marekha B. A., Koverga V. A., Chesneau E., Kalugin O. N., Takamuku T., Jedlovszky P., Idrissi A. Local structure in terms of nearest-neighbor approach in 1-butyl-3-methylimidazolium-based ionic liquids: Md simulations. *The Journal of Physical Chemistry B* 2016, *120* (22), 5029-5041. https://doi.org/10.1021/acs.jpcb.6b04066
32. Zahn S., Brehm M., Brüssel M., Hollóczki O., Kohagen M., Lehmann S., Malberg F., Pensado A. S., Schöppke M., Weber H., et al. Understanding ionic liquids from theoretical methods. *Journal of Molecular Liquids* 2014, *192* 71-76. https://doi.org/10.1016/j.molliq.2013.08.015
33. Abraham M. J., Murtola T., Schulz R., Páll S., Smith J. C., Hess B., Lindah E. Gromacs: High performance molecular simulations through multi-level parallelism from laptops to supercomputers. *SoftwareX* 2015, *1-2* 19-25. https://doi.org/10.1016/j.softx.2015.06.001
34. Bussi G., Donadio D., Parrinello M. Canonical sampling through velocity rescaling. *The Journal of Chemical Physics* 2007, *126* (1), 014101. https://doi.org/10.1063/1.2408420
35. Berendsen H. J. C., Postma J. P. M., Van Gunsteren W. F., Dinola A., Haak J. R. Molecular dynamics with coupling to an external bath. *The Journal of Chemical Physics* 1998, *81* (8), 3684-3684. https://doi.org/10.1063/1.448118
36. Essmann U., Perera L., Berkowitz M. L., Darden T., Lee H., Pedersen L. G. A smooth particle mesh ewald method. *The Journal of Chemical Physics* 1998, *103* (19), 8577-8577. https://doi.org/10.1063/1.470117
37. Allen P., Tildesley D. J. *Computer simulation of liquids*. Clarendon Press: Oxford, 1987. https://doi.org/10.1093/oso/9780198803195.001.0001
38. Mondal A., Balasubramanian S. Quantitative prediction of physical properties of imidazolium based room temperature ionic liquids through determination of condensed phase site charges: A refined force field. *Journal of Physical Chemistry B* 2014, *118* (12), 3409-3422. https://doi.org/10.1021/jp500296x
39. Mondal A., Balasubramanian S. A refined all-atom potential for imidazolium-based room temperature ionic liquids: Acetate, dicyanamide, and thiocyanate anions. *Journal of Physical Chemistry B* 2015, *119* (34), 11041-11051. https://doi.org/10.1021/acs.jpcb.5b02272
40. Koverga V. A., Korsun O. M., Kalugin O. N., Marekha B. A., Idrissi A. A new potential model for acetonitrile: Insight into the local structure organization. *Journal of Molecular Liquids* 2017, *233* 251-261. https://doi.org/10.1016/j.molliq.2017.03.025
41. Koverga V. A., Voroshylova I. V., Smortsova Y., Miannay F. A., Cordeiro M. N. D. S., Idrissi A., Kalugin O. N. Local structure and hydrogen bonding in liquid γ-butyrolactone and propylene car-

bonate: A molecular dynamics simulation. *Journal of Molecular Liquids* 2019, *287* 110912-110912. https://doi.org/10.1016/j.molliq.2019.110912
42. Canongia Lopes J. N., Deschamps J., Pádua A. A. H. Modeling ionic liquids using a systematic all-atom force field. *The Journal of Physical Chemistry B* 2004, *108* (6), 2038-2047. https://doi.org/10.1021/jp0362133
43. Canongia Lopes J. N., Pádua A. A. H. Molecular force field for ionic liquids composed of triflate or bistriflylimide anions. *The Journal of Physical Chemistry B* 2004, *108* (43), 16893-16898. https://doi.org/10.1021/jp0476545
44. Canongia Lopes J. N., Pádua A. A. H. Molecular force field for ionic liquids iii: Imidazolium, pyridinium, and phosphonium cations; chloride, bromide, and dicyanamide anions. *The Journal of Physical Chemistry B* 2006, *110* (39), 19586-19592. https://doi.org/10.1021/jp063901o
45. Ryckaert J. P., Bellemans A. Molecular dynamics of liquid n-butane near its boiling point. *Chemical Physics Letters* 1975, *30* (1), 123-125. https://doi.org/10.1016/0009-2614(75)85513-8
46. Bernardes C. E. S., Minas da Piedade M. E., Canongia Lopes J. N. The structure of aqueous solutions of a hydrophilic ionic liquid: The full concentration range of 1-ethyl-3-methylimidazolium ethylsulfate and water. *The Journal of Physical Chemistry B* 2011, *115* (9), 2067-2074. https://doi.org/10.1021/jp1113202
47. Hanke C. G., Lynden-Bell R. M. A simulation study of water−dialkylimidazolium ionic liquid mixtures. *The Journal of Physical Chemistry B* 2003, *107* (39), 10873-10878. https://doi.org/10.1021/jp034221d
48. Marekha B. A., Kalugin O. N., Idrissi A. Non-covalent interactions in ionic liquid ion pairs and ion pair dimers: A quantum chemical calculation analysis. *Physical Chemistry Chemical Physics* 2015, *17* (26), 16846-16857. https://doi.org/10.1039/C5CP02197A
49. Bernardes C. E. S. Aggregates: Finding structures in simulation results of solutions. *J. Comput. Chem.* 2017, *38* (10), 753-765. https://doi.org/10.1002/jcc.24735
50. Hess B. Determining the shear viscosity of model liquids from molecular dynamics simulations. *The Journal of Chemical Physics* 2002, *116* (1), 209-209. https://doi.org/10.1063/1.1421362
51. Macchieraldo R., Esser L., Elfgen R., Voepel P., Zahn S., Smarsly B. M., Kirchner B. Hydrophilic ionic liquid mixtures of weakly and strongly coordinating anions with and without water. *ACS Omega* 2018, *3* (8), 8567-8582. https://doi.org/10.1021/acsomega.8b00995
52. Weber H., Hollóczki O., Pensado A. S., Kirchner B. Side chain fluorination and anion effect on the structure of 1-butyl-3-methylimidazolium ionic liquids. *The Journal of Chemical Physics* 2013, *139* (8), 084502-084502. https://doi.org/10.1063/1.4818540
53. Doherty B., Zhong X., Gathiaka S., Li B., Acevedo O. Revisiting opls force field parameters for ionic liquid simulations. *Journal of Chemical Theory and Computation* 2017, *13* (12), 6131-6145. https://doi.org/10.1021/acs.jctc.7b00520
54. Humphrey W., Dalke A., Schulten K. Vmd: Visual molecular dynamics. *Journal of Molecular Graphics* 1996, *14* (1), 33-38. https://doi.org/10.1016/0263-7855(96)00018-5
55. Kalugin O. N., Voroshylova I. V., Riabchunova A. V., Lukinova E. V., Chaban V. V. Conductometric study of binary systems based on ionic liquids and acetonitrile in a wide concentration range. *Electrochimica Acta* 2013, *105* 188-199. https://doi.org/10.1016/j.electacta.2013.04.140
56. Vraneš M., Papović S., Tot A., Zec N., Gadžurić S. Density, excess properties, electrical conductivity and viscosity of 1-butyl-3-methylimidazolium bis(trifluoromethylsulfonyl)imide + γ-butyrolactone binary mixtures. *The Journal of Chemical Thermodynamics* 2014, *76* 161-171. https://doi.org/10.1016/j.jct.2014.03.025
57. Stoppa A., Hunger J., Buchner R. Conductivities of binary mixtures of ionic liquids with polar solvents. *Journal of Chemical & Engineering Data* 2009, *54* (2), 472-479. https://doi.org/10.1021/je800468h
58. Fu Y., Cui X., Zhang Y., Feng T., He J., Zhang X., Bai X., Cheng Q. Measurement and correlation of the electrical conductivity of the ionic liquid [bmim][tfsi] in binary organic solvents. *Journal of Chemical & Engineering Data* 2018, *63* (5), 1180-1189. https://doi.org/10.1021/acs.jced.7b00646
59. France-Lanord A., Grossman J. C. Correlations from ion pairing and the nernst-einstein equation. *Phys Rev Lett* 2019, *122* (13), 136001. https://doi.org/10.1103/PhysRevLett.122.136001

60. Marekha B. A., Kalugin O. N., Bria M., Buchner R., Idrissi A. Translational diffusion in mixtures of imidazolium ils with polar aprotic molecular solvents. *The Journal of Physical Chemistry B* 2014, *118* (20), 5509-5517. https://doi.org/10.1021/jp501561s

Received 05.09.2023 *Accepted 17.11.2023*

Д.С. Дударєв [*†], Я.В. Колесник[*], А. Ідріссі[†], О.М. Калугін[*]. Молекулярно-динамічне дослідження іонних рідин на основі імідазолію та молекулярних розчинників: мікроструктура та транспортні властивості

[*]*Харківський національний університет імені В.Н. Каразіна, хімічний факультет, майдан Свободи, 4, Харків, 61022, Україна*

[†]Університет Лілю, CNRS UMR 8516 -LASIRe - Laboratoire Avancé de Spectroscopie pour les Interactions la Réactivité et l'environnement, 59000 Ліль, Франція

Бінарні суміші, що складаються з іонних рідин при кімнатній температурі та апротонних диполярних розчинників, широко використовуються в сучасній електрохімії. Хоча ці системи демонструють максимуми електропровідності та інші особливості в розведених розчинах, підтверджені даними ЯМР і вібраційної спектроскопії, на сьогоднішній день відсутня теорія, яка могла б пояснити ці явища. У даній роботі методом молекулярно-динамічного моделювання досліджено дванадцять сумішей іонних рідин (IP) зокрема 1-бутил-3-метилімдазолію (C_4mim^+) з тетрафлуорборатом (BF_4^-), гексафлуорфосфатом (PF_6^-), трифлуорметансульфонатом (TFO^-) і біс(трифлуорметан)сульфонімідом ($TFSI^-$)), у поєднанні з молекулярними розчинниками, такими як ацетонітрил (AN), пропіленкарбонат (PC) або гамма-бутиролактон (γ-BL). Локальну структуру сумішей досліджували за допомогою функцій радіального розподілу (ФРР) та поточних координаційних чисел (ПКЧ), що виявили особливості поведінки в системах з AN та $TFSI^-$. Для системи з $TFSI^-$ спостерігалися два піки на ФРР з однаковою інтенсивністю. Було досліджено взаємне розташування катіонів та аніонів, яке відповідає міжатомним відстаням, що спостерігаються на ФРР: вони відображають конфігурації, коли атом азоту аніону знаходиться поблизу імідазолієвого кільця, і коли атом азоту $TFSI^-$ безпосередньо не взаємодіє з кільцем, натомість це роблять атоми кисню. Катіон-аніонні координаційні числа змінювалися для сумішей з AN від ~1,2 до ~3,6, для PC – від 0,6 до 3,0 та для γ-BL – від 0,8 до 3,1 зі збільшенням молярної частки IP. Крім того, аналіз асоціації був проведений з використанням двох різних критеріїв відстані. Результати показали утворення великих кластерів при приблизно 0,15, 0,20 та 0,25 мольних частках іонної рідини для AN, PC та γ-BL відповідно, на основі першого критерію. Однак цей критерій має тенденцію переоцінювати ступінь агрегації. На відміну від нього, другий, суворіший критерій вказує, що утворення великих агрегатів починається при мольних частках іонної рідини, подібних до тих, де експериментальні криві провідності досягають максимуму. Для аналізу транспортних властивостей були отримані коефіцієнти дифузії всіх компонентів та в'язкість для всіх бінарних сумішей. Коефіцієнти дифузії добре узгоджуються з експериментальними даними.

Ключові слова:. *1-бутил-3-метилімдазолій, іонні рідини, апротонні диполярні розчинники, локальна структура, транспортні властивості, іонна агрегація*

Надіслано до редакції 05.09.2023 *Прийнято до друку 17.11.2023*